Supporting Information

Wang et al. 10.1073/pnas.1404680111

SI Experimental Procedures

Plant Materials and Growth Conditions. The *spx1* mutant (M0101661), identified from the Taiwan Rice Insertional Mutants Database (http://trim.sinica.edu.tw/), harbors a T-DNA insertion in the second exon of *SPX1*. The *spx2* mutant (PFG_3A-02559), bought from the Rice T-DNA Insertion Sequence Database (http://cbi.khu.ac.kr/RISD_DB.html), harbors a T-DNA insertion in the second exon of *SPX2*. Homozygous *spx1* and *spx2* mutants were identified by PCR amplification of the T-DNA flanking regions; RT-PCR detection of mRNA for corresponding genes demonstrated that *spx1* and *spx2* are loss-of-function mutations. The *spx1* and *spx2* mutants were introgressed into the *japonica* rice cultivar Nipponbare through three successive crosses to Nipponbare. The *spx1spx2* double mutant was obtained by crossing *spx2* to *spx1*. The primers used for the identification of mutants are listed in Table S1. Hydroponic experiments were conducted using rice culture solution with NaH_2PO_4 [0, 10, or 200 μM phosphate (Pi), as indicated]. The nutrient solution was adjusted to pH 5.5 using 1 M NaOH and replaced every 2 d. Experiments were carried out in a greenhouse with a 12-h day (30 °C)/12-h night (22 °C) photoperiod, ∼200 $\mu mol \cdot m^{-2} \cdot s^{-1}$ photon density, and ∼60% humidity.

Complementation of *spx1* and *spx2* Mutants. For complementation of the *spx1* and *spx2* mutants, genomic fragments containing the promoter, 5′ UTR, and full-length sequences coding SPX1 and SPX2, respectively, were cloned and inserted into the pBI101.3 vector (1). Constructs for *spx1* and *spx2* complementation were introduced into mutants using *Agrobacterium*-mediated transformation. Primers used are listed in Table S1.

Yeast Two-Hybrid Assays. The Matchmaker GAL4 two-hybrid system (Clontech) was used for yeast two-hybrid assays. Full-length and truncation derivatives of *SPX1* and *SPX2* (*SPX1*, *SPX2*, *SPX1-N168*, and *SPX2-N164*) were cloned into pGADT7, and the C terminus of the *PHR2* coding sequence (*PHR2-C196*) was cloned into pGBKT7. Primers used are listed in Table S1. Constructs were cotransformed in the AH109 yeast strain. Medium lacking Leu, Trp, His, and Ade was used for selection.

Coimmunoprecipitation Assays. The *6×MYC* coding sequence amplified from the 35S-MYC vector (2) was cloned into 35S-pCAMBIA1300-mod (3) to generate the 35S-MYC-pCAMBIA1300-mod vector. Full-length and truncation derivatives of *SPX1* and *SPX2* (*SPX1*, *SPX2, SPX1-N168*, and *SPX2-N164*) were cloned into the 35S-MYC-pCAMBIA1300-mod vector. Full-length and truncated derivatives of *PHR2* (*PHR2*, *PHR2-N230*, and *PHR2-C196*) were cloned into *35S-FLAG* (4). Primers used are listed in Table S1. The constructs were transiently expressed in tobacco leaves by *Agrobacterium* infiltration. The coimmunoprecipitation assays were performed as described (5). Anti-FLAG magnetic beads (Sigma) were used to immunoprecipitate protein complexes, and proteins were detected using an ECL reagent (Millipore) and the ChemDoc XRS system (Bio-Rad).

Bimolecular Fluorescence Complementation Assays. Full-length *SPX1* and *SPX2*, as well as full-length *PHR2* and the C terminus of *PHR2* (*PHR2* and *PHR2-C196*), were cloned into C- or N-terminal fragments of YFP vectors (6). Primers used are listed in Table S1. The resulting constructs were transiently expressed in tobacco leaves by *Agrobacterium* infiltration. YFP fluorescence of tobacco leaves was assayed 3 d postinfiltration under a Zeiss LSM710 confocal microscope.

Subcellular Localization Analysis. For subcellular localization analysis, truncated derivatives of *SPX1* and *SPX2* were cloned into 35S-mGFP vector (1). Primers used are listed in Table S1. The resulting in-frame fusion constructs were transformed in rice protoplasts for examination of GFP images by confocal microscopy. The 35S-mGFP vector was used as a control. Rice protoplast preparation and transformation were as described (1).

Development of Genetic Materials. The *phr2spx1spx2* triple mutants were developed by crossing *phr2* (1) to the *spx1spx2* double mutant. To generate transgenic plants overexpressing *SPX2*, *SPX1-N168*, and *SPX2-N164*, full-length *SPX2* and truncation derivatives of *SPX1* and *SPX2* were cloned into 35S-pCAMBIA1300-mod to generate *35S-SPX2*, *35S-SPX1-N168*, and *35S-SPX2-N164*. These vectors were then introduced into WT rice (Nipponbare) using the *Agrobacterium*-mediated transformation method. *OxPHR2/OxSPX2*, *OxPHR2/OxSPX1-N168*, and *OxPHR2/OxSPX2-N164* were obtained by crossing *OxSPX2*, *OxSPX1-N168-1*, and *OxSPX2-N164-2* to *OxPHR2* (7), respectively.

RNA Isolation, RT-PCR, and Quantitative RT-PCR Analysis. RNA isolation, RT-PCR and quantitative RT-PCR (qRT-PCR) analyses were performed as described (8). Primers used for RT-PCR and qRT-PCR analyses are listed in Table S1.

Microarray Analysis. Fourteen-day-old plants growth under +phosphorus (P) conditions were treated with +P or −P for another 7 d, and shoots of plants from three biological repeats were sampled for Affymetrix microarray analysis. Microarray and data analysis were performed as described (9). A robust multiarray analysis algorithm was used for summarization of background correction, normalization, and expression levels. Differential expression analysis was performed with the Bayes *t*-statistics using Linear Models for Microarray Data (Limma) software. *P* values were corrected for multiple testing using the Benjamini–Hochberg method (false discovery rate). Genes were considered to be differentially expressed if corrected *P* values were <0.05, and only genes with a signal log ratio more than 1 or less than −1 were considered for further analysis.

Measurement of Anthocyanin. Measurement of anthocyanin was performed as described by Jiang et al. (10). Anthocyanin was extracted from the second and third leaves (from the top) of 30-d-old WT, *spx1*, *spx2*, and *spx1spx2* plants grown in +P culture.

ChIP-PCR Analysis. To generate *PHR2pro-PHR2-FLAG* transgenic plants, the *3×FLAG* coding sequence was amplified from *35S-FLAG* to generate FLAG-pBI101.3. A 4.3-kb genomic fragment containing the full-length coding region of *PHR2* was cloned into FLAG-pBI101.3 between the BamHI and KpnI sites. A 2.9-kb genomic fragment containing the promoter and 5′ UTR of *PHR2* was cloned upstream of the *PHR2* coding region between the SalI and BamHI sites. The *PHR2pro-PHR2-FLAG* construct was introduced into the *phr2* mutant (1). The *spx1spx2* plants harboring *PHR2pro-PHR2-FLAG* for ChIP-PCR were obtained by crossing *spx1spx2* plants with *PHR2pro-PHR2-FLAG* plants. ChIP-PCR assays were performed as described (11). Primers used for the constructs and ChIP-PCR are listed in Table S1.

In Vitro Pull-Down Assay. Full-length *SPX1* and *SPX2* were cloned into pGEX-4T-1 (GE Healthcare). Primers used are listed in Table S1. Recombinant proteins produced in *Escherichia coli* were purified using Glutathione Sepharose 4 Fast Flow (GE Healthcare). PHR2-His was purified as described (8). Pull-down

assays were performed as described (5). In brief, pull-down buffer [10 mM Tris·HCl (pH 7.5), 50 mM KCl, 5 mM $MgCl_2$, 1 mM DTT, 0.05% Nonidet P-40, and 2.5% (vol/vol) glycerol] was prepared, and NaH_2PO_4 solution was added or not added to pull-down buffer to 15 mM Pi as indicated. Prokaryotic expressed PHR2-His, GST-SPX1, GST-SPX2, various concentrations of 4× PHOSPHATE STARVATION RESPONSE REGULATOR 1 (PHR1)-binding sequence (P1BS) probe and nickel-nitrilotriacetic acid agarose (Qiagen) were then added into buffer and incubated at 4 °C for 2 h. Pull-down proteins were washed with buffer [50 mM Tris·HCl (pH 7.50), 300 mM NaCl, and 40 mM imidazole) before resolution in 10% (wt/vol) SDS/PAGE and immunoblot analysis using anti-GST antibody (Sigma). Proteins were detected using ECL (Millipore) and the ChemDoc XRS system (Bio-Rad).

EMSA. PHR2-His, GST-SPX1, and GST-SPX2 proteins were purified as above. The SPX domains of *SPX1* and *SPX2* (*SPX1-N168* and *SPX2-N164*) were cloned into pGEX-4T-1 (GE Healthcare), and recombinant proteins were purified as the full length of *SPX1* and *SPX2*. Primers used are listed in Table S1. For nuclear protein EMSA, 20-d-old WT, *phr2*, *spx1*, *spx2*, and *spx1spx2* cultured under Pi-sufficient conditions were sampled, and nuclear proteins were extracted using a Plant Nuclei Isolation/Extraction Kit (Sigma) with 3% (vol/vol) of Triton X-100 added to the extraction buffer. DNA fragments containing P1BS of *SPX1*, *SPX2*, and *IPS1* promoters or 5′ UTR were amplified using biotin-labeled primers (Table S1) and purified with a PCR purification kit (Qiagen). The 4× P1BS probe containing four tandem copies of *P1BS* was generated as described (9). EMSA was performed with a LightShift Chemiluminescent EMSA Kit (Pierce). Pi (NaH_2PO_4 solution, pH 7.5) was added to EMSA buffer to a final concentration as indicated. For nuclear protein EMSA, 500 ng of nuclear protein of each sample and 100 fmol of biotin-labeled primers were used. Migration of biotin-labeled probes was detected using ECL (Pierce) and ChemDoc XRS (Bio-Rad). Immunoblot analysis using Anti-Histone H3 antibody (Abcam) was used as a loading control.

Immunobloting Analysis. To obtain *SPX1pro-SPX1-MYC* and *SPX2pro-SPX2-MYC* transgenic plants, the *6×MYC* coding sequence (amplified from 35S-MYC) was used to replace the *GFP* coding sequence in GFP-pBI101.3 (12) to generate the MYC-pBI101.3 vector. Genomic fragments containing the promoter, 5′ UTR, and full-length coding region of *SPX1* and *SPX2* were cloned into MYC-pBI101.3. Constructs were introduced into corresponding mutants by *Agrobacterium*-mediated transformation. Primers used are listed in Table S1. For immunoblot analysis of SPX1 and SPX2, *SPX1pro-SPX1-MYC* and *SPX2pro-SPX2-MYC* seedlings were sampled and ground in liquid nitrogen and dissolved in protein lysis buffer [50 mM Tris·HCl (pH 7.5), 150 mM NaCl, 1 mM EDTA, 10% (vol/vol) glycerol, 1% Triton X-100, 1 mM PMSF, 10 μM MG132, and complete protease inhibitor (Roche)]. Total protein (40 μg) of each sample was separated on SDS/PAGE. Immunoblot analysis was performed using rabbit anti-MYC antibody to detect SPX1-MYC and SPX2-MYC.

1. Chen J, et al. (2011) OsPHF1 regulates the plasma membrane localization of low- and high-affinity inorganic phosphate transporters and determines inorganic phosphate uptake and translocation in rice. *Plant Physiol* 157(1):269–278.
2. Hong GJ, Xue XY, Mao YB, Wang LJ, Chen XY (2012) *Arabidopsis* MYC2 interacts with DELLA proteins in regulating sesquiterpene synthase gene expression. *Plant Cell* 24(6):2635–2648.
3. Wang C, et al. (2009) Involvement of OsSPX1 in phosphate homeostasis in rice. *Plant J* 57(5):895–904.
4. Menon S, Rubio V, Wang X, Deng X-W, Wei N (2005) Purification of the COP9 signalosome from porcine spleen, human cell lines, and *Arabidopsis thaliana* plants. *Methods Enzymol* 398:468–481.
5. Feng S, et al. (2008) Coordinated regulation of *Arabidopsis thaliana* development by light and gibberellins. *Nature* 451(7177):475–479.
6. Shen Q, et al. (2011) Tomato SlSnRK1 protein interacts with and phosphorylates βC1, a pathogenesis protein encoded by a geminivirus β-satellite. *Plant Physiol* 157(3): 1394–1406.
7. Zhou J, et al. (2008) *OsPHR2* is involved in phosphate-starvation signaling and excessive phosphate accumulation in shoots of plants. *Plant Physiol* 146(4):1673–1686.
8. Liu F, et al. (2010) OsSPX1 suppresses the function of OsPHR2 in the regulation of expression of *OsPT2* and phosphate homeostasis in shoots of rice. *Plant J* 62(3): 508–517.
9. Bustos R, et al. (2010) A central regulatory system largely controls transcriptional activation and repression responses to phosphate starvation in *Arabidopsis*. *PLoS Genet* 6(9):e1001102.
10. Jiang C, Gao X, Liao L, Harberd NP, Fu X (2007) Phosphate starvation root architecture and anthocyanin accumulation responses are modulated by the gibberellin-DELLA signaling pathway in Arabidopsis. *Plant Physiol* 145(4):1460–1470.
11. Saleh A, Alvarez-Venegas R, Avramova Z (2008) An efficient chromatin immunoprecipitation (ChIP) protocol for studying histone modifications in *Arabidopsis* plants. *Nat Protoc* 3(6):1018–1025.
12. Kang B, et al. (2013) OsCYP2, a chaperone involved in degradation of auxin-responsive proteins, plays crucial roles in rice lateral root initiation. *Plant J* 74(1): 86–97.

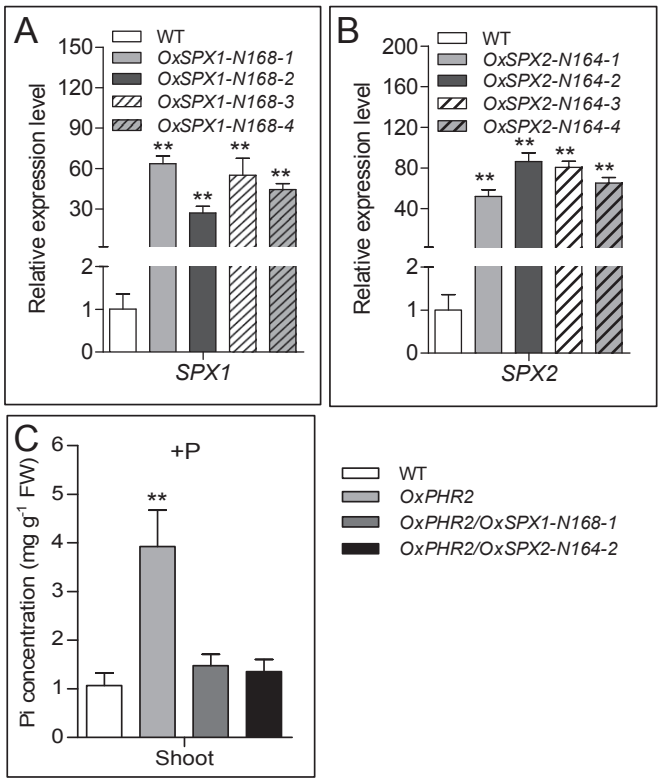

Fig. S1. Development of transgenic plant lines overexpressing functional *SPX1-N168* and *SPX2-N164,* which counteract PHR2 function. (*A*) qRT-PCR analysis of *SPX1* expression in WT and four transgenic lines overexpressing *SPX1-N168* (*OxSPX1-N168-1* to *OxSPX1-N168-4*). (*B*) qRT-PCR analysis of *SPX2* expression in WT and four transgenic lines overexpressing *SPX2-N164* (*OxSPX2-N164-1* to *OxSPX2-N164-4*). (*C*) Cellular Pi concentrations in shoots of 30-d-old WT, *OxPHR2*, *OxPHR2/OxSPX1-N168-1*, and *OxPHR2/OxSPX2-N164-2* plants in +P (200 μM Pi) conditions. FW, fresh weight. Data show mean + SD ($n = 3$ for *A* and *B*, $n = 5$ for *C*). Data significantly different from the WT control are indicated (**$P < 0.01$, Student *t* test).

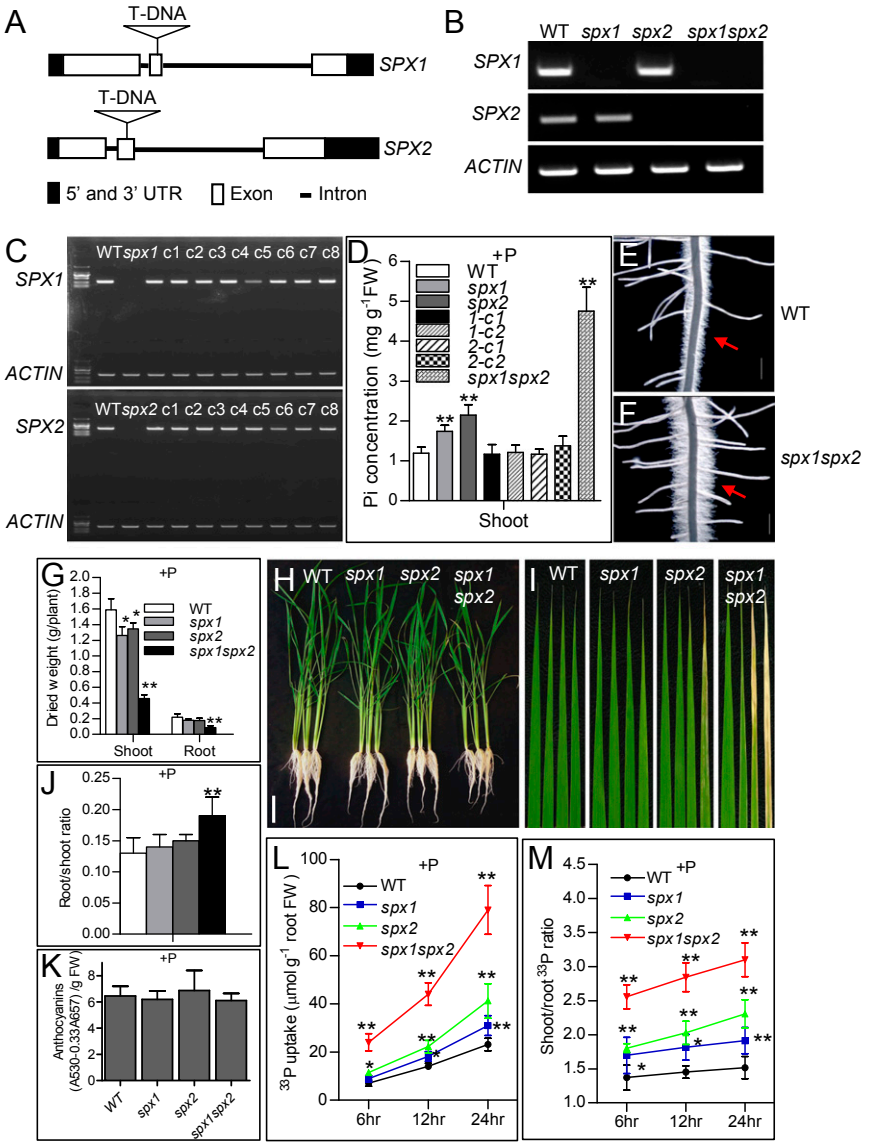

Fig. S2. Isolation of *spx1* and *spx2* mutants and phenotypes of *spx1*, *spx2*, and the double-mutant *spx1spx2*. (*A*) Scheme of the T-DNA insertional mutants *spx1* (M0101661) and *spx2* (PFG_3A-02559). The T-DNA insertions in the second exon of *SPX1* and *SPX2* are shown as triangles. Semi–qRT-PCR analysis of *SPX1* and *SPX2* expression in WT, *spx1*, *spx2*, and *spx1spx2* double-mutant plants (*B*) and lines for each complemented with WT *SPX1* and *SPX2* [complementation (c)1 to c8] (*C*). (*D*) Shoot cellular Pi concentrations in 30-d-old WT, *spx1*, *spx2*, *1-c1*, *1-c2*, *2-c1*, *2-c2*, and *spx1spx2* plants grown in Pi-sufficient (+P, 200 μM Pi) conditions. Root hairs of 4-d-old seedlings of WT (*E*) and *spx1spx2* double-mutant (*F*) plants grown in +P culture. (Scale bar: 1 mm.) Arrows point to the root hairs. (*G*) Dried weight of 30-d-old WT, *spx1*, *spx2*, and *spx1spx2* plants grown in +P culture. (*H*) Phenotype of 30-d-old WT, *spx1*, *spx2*, and *spx1spx2* plants grown in +P culture. (Scale bar: 10 cm.) (*I*) Enlarged views of leaf tips of plants in *H*. (*Left* to *Right*) The first, second, third, and fourth leaves are shown. Root-to-shoot ratio (*J*) and anthocyanin content (*K*) of 30-d-old WT, *spx1*, *spx2*, and *spx1spx2* plants grown in +P culture are shown. ^{33}P uptake ability (*L*) and shoot/root ^{33}P ratio (*M*) of WT, *spx1*, *spx2*, and *spx1spx2* plants under +P conditions are shown. The 20-d-old plants were transferred to a 200-μM Pi solution culture containing [^{33}P] KH_2PO_4 over a period of 24 h. Data show (*D*, *G*, *J*, and *K*) mean + SD and (*L* and *M*) mean ± SD ($n = 5$ for *D*, *G*, and *J*–*M*). Data significantly different from the WT control are indicated (*$P < 0.05$, **$P < 0.01$; Student *t* test).

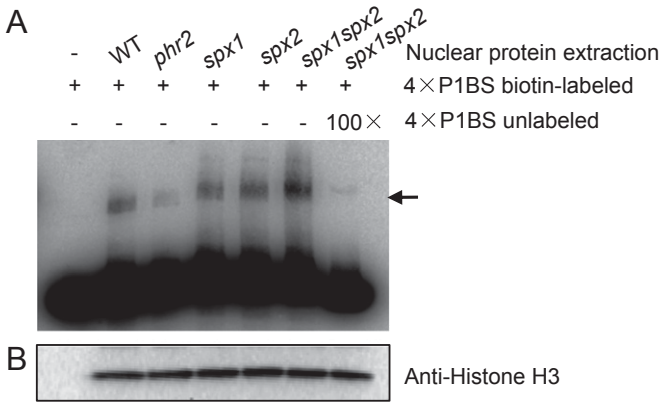

Fig. S3. KO of *SPX1* and *SPX2* enhances the P1BS binding ability of PHR2, as revealed by EMSA using nuclear extracted proteins. (*A*) Results of EMSA using nuclear extracted proteins. (*B*) Western blot of Anti-Histone H3 antibody to show the equal loading of the nuclear proteins used in EMSA. Twenty-day-old seedlings of WT, *phr2*, *spx1*, *spx2*, and *spx1spx2* plants were used to isolate nuclear proteins for the EMSA assay. The PHR2–DNA complex is indicated by a black arrow.

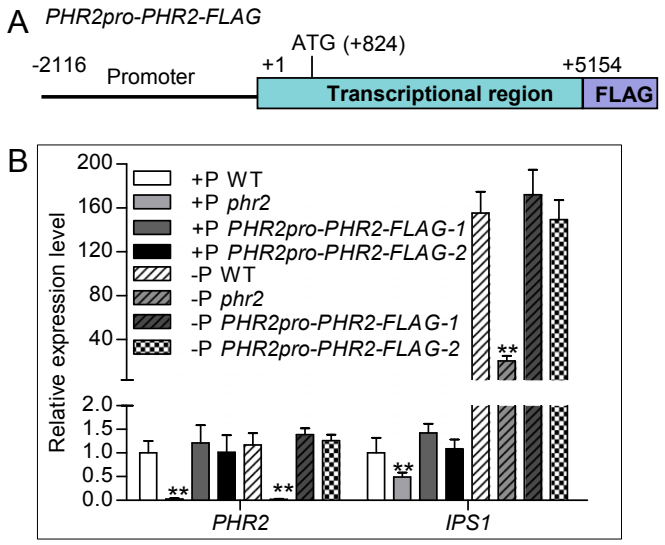

Fig. S4. Complementation of *phr2* by *PHR2pro-PHR2-FLAG* fusions. (*A*) Scheme of *PHR2pro-PHR2-FLAG* constructs. Numbers above the promoter (black line) and transcriptional region (light blue bar) indicate the position from the *PHR2* transcription start site. (*B*) qRT-PCR analysis of *PHR2* and *IPS1* expression in roots of WT, *phr2*, and two transgenic plants expressing *PHR2pro-PHR2-FLAG* in +P (200 μM Pi) and −P conditions. Data show mean + SD ($n = 3$). Data significantly different from WT controls are indicated (**$P < 0.01$, Student *t* test).

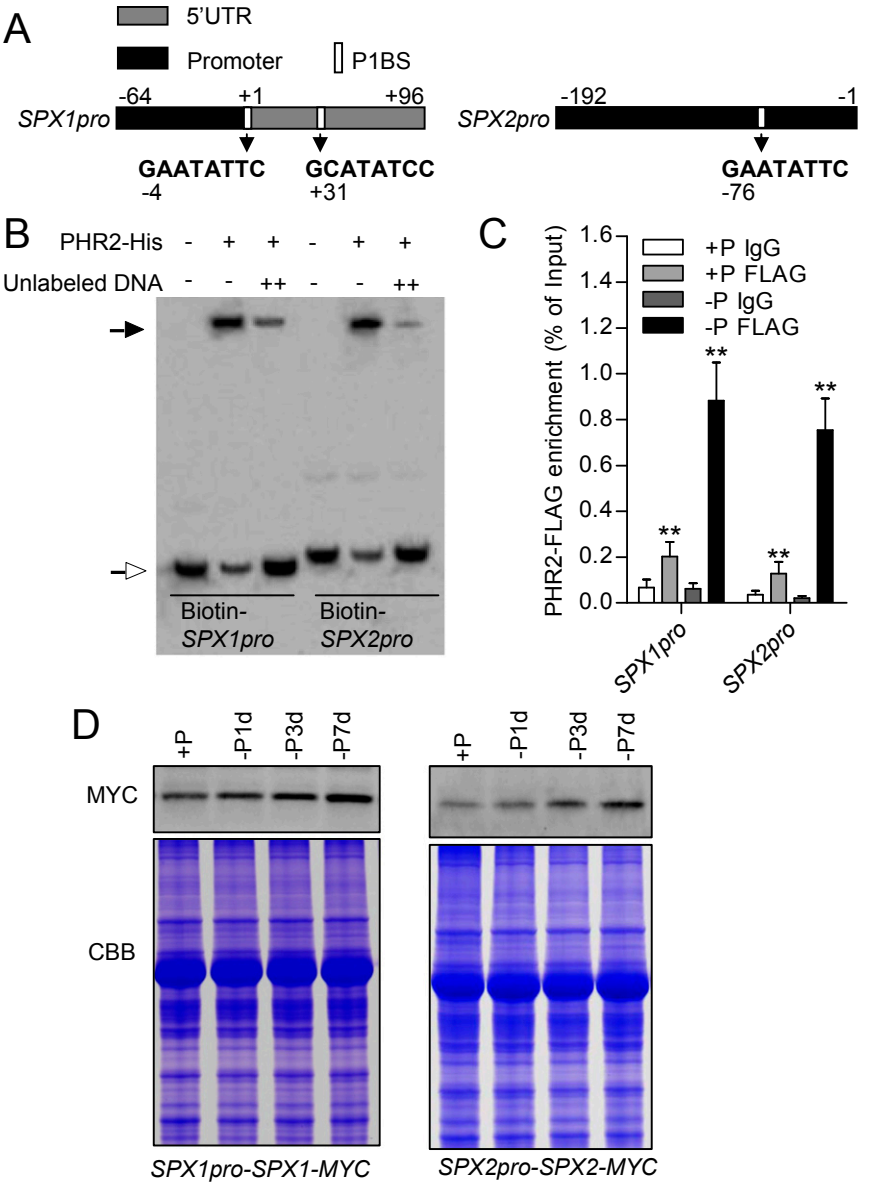

Fig. S5. PHR2 directly up-regulates *SPX1* and *SPX2*, and the SPX1 and SPX2 proteins are accumulated in −P conditions. (*A*) Diagram of P1BS positions in the *SPX1* 5′ UTR and in the *SPX2* promoter used for ChIP-PCR and EMSA analyses. Numbers above the promoters indicate the position from transcription start site of each gene. (*B*) EMSA analysis to test PHR2 binding to the P1BS motifs in *A*. The PHR2–DNA complex and free DNA are indicated by black and white arrows, respectively. ++, 100-fold molar excess of unlabeled probe. (*C*) ChIP-PCR analysis of PHR2 binding to the P1BS motifs in *A* in +P and −P conditions in vivo. Chromatin from *PHR2pro-PHR2-FLAG* seedlings was immunoprecipitated with nonspecific IgG or anti-FLAG antibody (FLAG). The histogram shows PHR2-FLAG enrichment (% of input) of the *SPX1* and *SPX2* promoters. Data show mean + SD ($n = 3$). Data significantly different from the IgG control are indicated (**$P < 0.01$, Student *t* test). (*D*) Immunoblot analyses of SPX1 and SPX2 protein levels in −P conditions. Ten-day-old plants harboring *SPX1pro-SPX1-MYC* or *SPX2pro-SPX2-MYC* grown in +P conditions were transferred to −P conditions (no Pi) for 7 d and sampled at the times indicated. Anti-MYC antibody (MYC) was used to detect SPX1 and SPX2. (*Lower*) Coomassie brilliant blue (CBB)-stained blots are shown as loading controls.

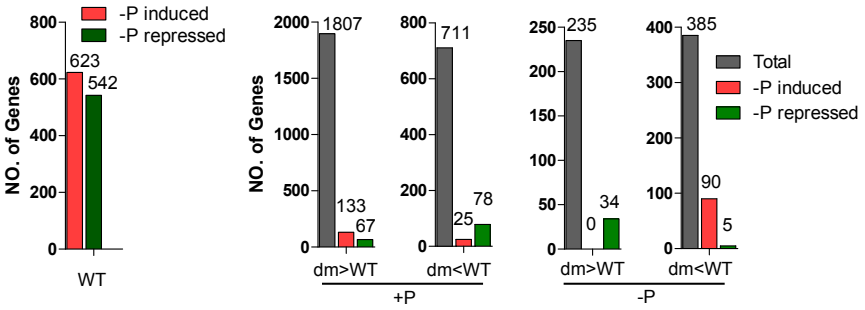

Fig. S6. Diagram showing transcriptomic analysis of WT and *spx1spx2* [double-mutant (dm)] plants grown for 14 d and then treated with +P (200 μM Pi) or −P (0 μM Pi) for 7 d. The total number of genes induced or repressed by Pi starvation in WT plants is shown above the bars (2× cutoff, false discovery rate of 0.05). The number of genes whose expression is higher (dm > WT) or lower (dm < WT) in *spx1spx2* plants than in WT plants in each growth condition is also shown. The number of Pi starvation-responsive genes (−Pi induced and −Pi repressed) among them is indicated. Three biological replicates were analyzed.

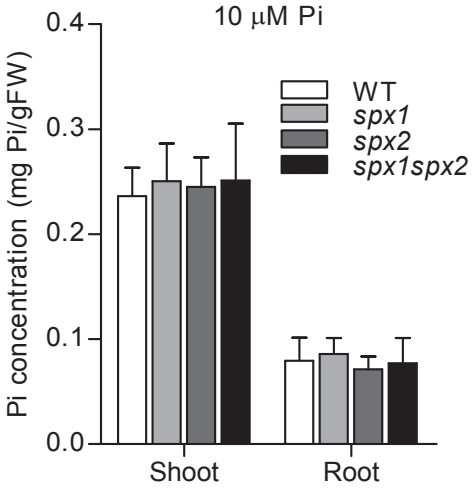

Fig. S7. Shoot and root cellular Pi concentrations in 30-d-old WT, *spx1*, and *spx2* single mutant plants and *spx1spx2* double-mutant plants grown in Pi-deficient (10 μM Pi) conditions. Data show mean + SD ($n = 5$).

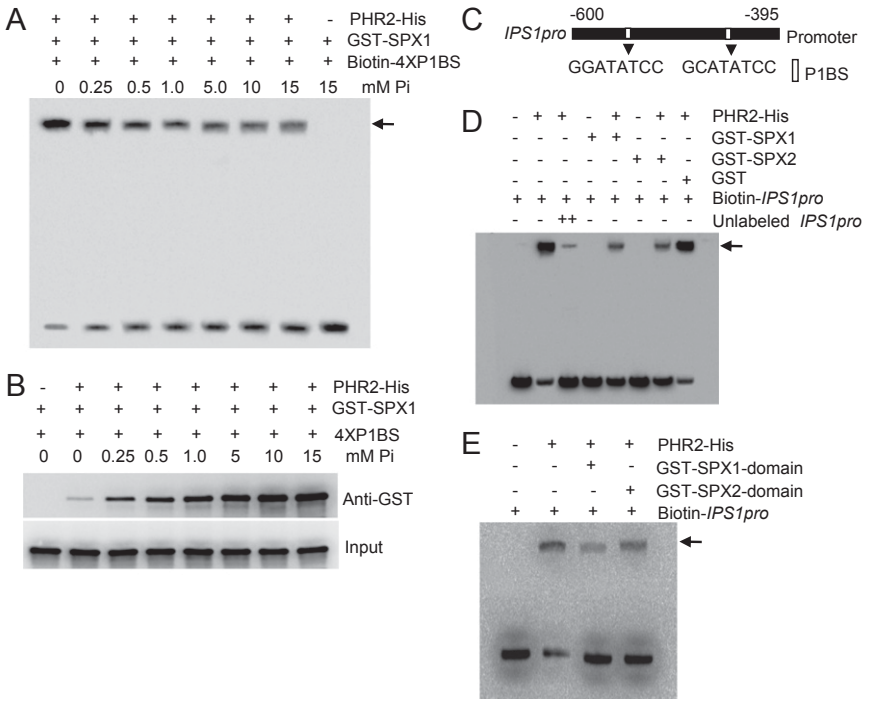

Fig. S8. Negative effects of SPX1 on PHR2-binding ability are responsive to the Pi concentration, and SPX domains inhibit PHR2 binding to the P1BS motif in the presence of Pi. (*A*) EMSA analysis to test the SPX1 inhibition of PHR2 binding to the P1BS motifs under various Pi concentrations. EMSA was performed with PHR2-His (50 ng per lane), GST-SPX1 protein (250 ng per lane), and biotin-labeled 4× P1BS probe (100 fmol per lane). (*B*) Pull-down assays to test the SPX1 inhibition of PHR2 binding to the P1BS motifs under various Pi concentrations. Purified bacterially expressed PHR2-His (50 ng), 4× P1BS probe (100 fmol per lane), and GST-SPX1 protein (250 ng) were used in each lane, with various Pi concentrations. GST-SPX1 was detected using anti-GST. (*C*) Diagram of *IPS1* promoter regions, including P1BS motifs for EMSA. Numbers above the promoters indicate positions before the transcription start site. The sequence and position of each P1BS motif are shown (black arrowhead). (*D*) SPX1 and SPX2 inhibit PHR2 binding to the P1BS motif in +P (15 mM Pi), as indicated by EMSA. EMSA was performed with PHR2-His (50 ng per lane), GST-SPX1 or GST-SPX2 protein (250 ng per lane), and biotin-labeled *IPS1* promoter (*IPS1pro*). GST (250 ng per lane) was used as a control. ++, 100-fold molar excess of unlabeled probe. (*E*) SPX domains of SPX1 and SPX2 inhibit PHR2 binding to the P1BS motif in +P (15 mM Pi), as indicated by EMSA. Purified bacterially expressed GST-SPX1-N168 or GST-SPX2-N164 was used (250 ng per lane). The PHR2–DNA complex is indicated (black arrow).

Other Supporting Information Files

Table S1 (DOC)